ELSEVIER

Sensors and Actuators A 94 (2001) 95–101

SENSORS AND ACTUATORS A PHYSICAL

www.elsevier.com/locate/sna

On-line measurement of the straightness of seamless steel pipes using machine vision technique

R.S. Lu[a], Y.F. Li[a,*], Q. Yu[b]

[a]Department of Manufacturing Engineering and Engineering Management, City University of Hong Kong, Kowloon, Hong Kong
[b]Tinjin University, Tinjin, China

Accepted 17 June 2001

Abstract

In this paper, on-line and real-time laser visual alignment measurement technique is studied to measure the spatial straightness of large objects. The basic principle of the visual alignment measurement is detailed. The mathematics models of visual sensor, measurement system and their calibrations are presented. Based on the technique, an experiment system is developed and the straightness of a 1500 mm long seamless steel pipe is inspected. The experiment results show that the measurement technique can achieve total on-line measurement and it offers high precision and stability, which is of practical importance for the application.

Keywords: Visual alignment; Straightness; On-line measurement; Calibration

1. Introduction

Straightness is of critical importance for guaranteeing the quality of the screw threads machined at the ends seamless steel pipes. In order to monitor the product quality in product lines, 100% on-line measurement is required. Here, the straightness and diameter of seamless steel pipes over 10 meter long need to be inspected [1], with required straightness tolerances of <3 mm over the whole length. So far, no satisfactory method has been in practical use to solve the on-line automatic measurement of the straightness. Therefore, the straightness evaluation has to be accomplished manually by operators. This not only results in low measurement speed, but also makes the production quantity subject to human errors.

Over the years, different measurement methods for the related applications have been explored. These include the use of alignment telescope, jig transits, optical levels, the engineering theodolite and so on [2,3]. However, none of these are directly suitable for the 100% on-line measurement of the spatial straightness of large workpieces. Junichi et al. [4] used laser beam to obtain the straightness by moving target or mirror along the measured line or the measured central axis. However, there are two detrimental factors for the laser datum stability. One is the air flow in the beam path. The effect of air flow can be reduced by putting a comer (tube) around the beam path for small measurement ranges. However, for large objects, the efficiency of this method is not apparent. The other problem is the drift of the beam which is caused by "beam dancing" due mainly to the thermal deformation of the parts of the laser. The low drift of 3 nm over the working distance of about 200 mm can be expected by stabilization using water cooling for the laser tube. However, this stability is not sufficient for the measurement of straightness of longer parts such as the working distance up to 1 m [4]. In order to implement the straightness measurement method for a large object with multi-point displacements, Sasaki et al. [5] also used laser beam as the straightness reference. The only difference from the previously mentioned one is that the detector consists of four-cell type photodiodes inside a Si micromesh structure. The direction or the wave front of the reference laser beam is not disturbed, as sensor absorbs only some of the incident photons and transmits the remainder down stream. However, this method is still subject to the influence of environmental factors. Furthermore, it cannot be used directly for non-contact measurements. Parallel white light beam method was also attempted [6]. This method is not subject to the above detrimental effects, but like the Junichi's method, it cannot implement the non-contact measurement, since during the measurement, the moved target or reflection mirror

* Corresponding author. Tel.: +852-2788-8410; fax: +852-2788-8423.
E-mail address: meyfli@cityu.edu.hk (Y.F. Li).

0924-4247/01/$ – see front matter
PII: S0924-4247(01)00683-5

must be used. Herrmannsfeldt et al. [7] developed a zone plate method for straightness measurement. In this method, a system of large rectangular Fresnel lenses was used in the laser alignment system for the SLAC 2-mile accelerator. The alignment system consists of a He–Ne laser light source, a photoelectric detector, and the lenses, one of which is located at each of the 297 points which are to be aligned. Each lens has the proper focal length to focus the laser to a point image at the detector. This method suffers from the same drawbacks as above. These methods can only be used for off-line spot check of large object's straightness. They are not suitable for 100% on-line non-contact automatic measurement of the straightness required here.

With the advancement of machine vision technology, visual gauging or inspection technique based on off-the-shelf charge coupled device (CCD), semiconductor laser, image grabber and image processing device, is becoming a an alternative for 100% on-line measurement in industrial applications. This method offers the desired properties of being non-contact, with proper precision, high speed and easy to operate. In this paper, we develop a laser visual alignment measuring technique to implement 100% on-line and non-contract measurement of straightness of large-scale object for the inspection of seamless steel pipe's straightness.

In Section 2, we introduce the fundamentals of the visual alignment system and its mathematic modeling. Then we describe in Section 3 how to obtain the coordinates of the centers of elliptical arc via the visual sensing. In Section 4, the calibration of the measurement system is given. Finally, in Section 5, this novel method is verified by experiments in the straightness measurement of a seamless steel pipe with 1500 mm length.

2. Measuring principle and system modeling

The measurement of straightness refers to that of the 3D coordinates of the points in the central axes of an object [8]. Therefore, as long as there are sufficient numbers of measured points along the axes of a workpiece, its straightness can be estimated. The key problem in the measurement is how to measure the 3D coordinates of the points along the measured line. The method we used to measure the straightness of the axis line of an external cylinder is illustrated in Fig. 1. Several laser visual sensors are placed along the axis to be measured. The laser beam emitted from each semiconductor laser device (LD) in the sensor is magnified by cylinder lens and transformed into a light plane, resulting in an ellipse arc when intersecting the axes' external surface. The images of the ellipse arcs sensed by the CCD cameras are transmitted to the image grabber through multiplexers controlled by the computer where they are digitized and stored in the frame memory. Thus, the 3D world coordinate of arc center in coordinate system X_w, Y_w, Z_w can be computed in the image processing. Then the straightness is estimated by an algorithm giving all the arc center coordinates.

As shown in Fig. 1, the visual alignment measurement system is a multi-sensor measurement system. The straightness is obtained on the basis of each sensor's measurement result. In order to obtain the measurement results, the measurement principle of each single sensor must be known. Fig. 2 illustrates this, where the model of CCD camera adopted is a pin-hole projection model [9,10].

In Fig. 2, the image coordinate system is O–XY, where O represents its origin that is the intersection of the image plane with the optical axis of the CCD camera. Here, X is chosen parallel to the rows of the CCD pixel array. The camera coordinate system is o–xyz, with point o coinciding with the optical center of the camera, at a distance f to the image plane. Here, f represents the effective focal length of the camera. The z-axis coincides with its optical axis, and the x- and y-axis are parallel to the X- and Y-axis, respectively. The sensor coordinate system is defined on the light plane. The world coordinate system is built in a similar way. Point p is an arbitrary point on the arc formed by the intersection of the light plane with the cylinder p(x_s, y_s, 0) is the coordinate of the point p in the sensor coordinate system. p(x, y, z) is the coordinate of p in the camera coordinate system, and p(x_w, y_w, z_w) is that of p in the world coordinate system. The ideal (undistorted) coordinate of the point p in the image

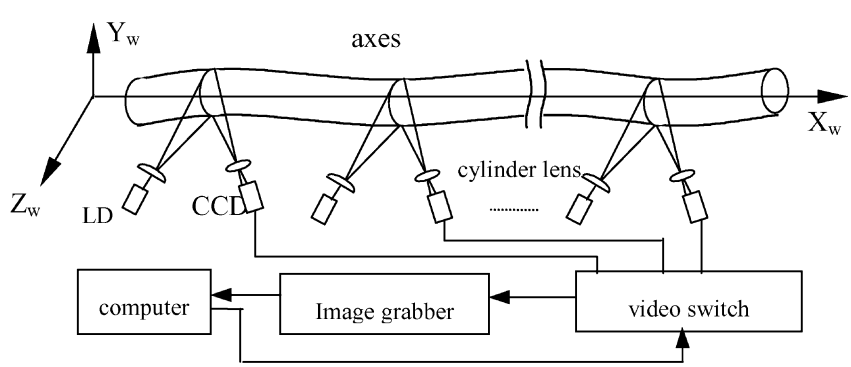

Fig. 1. The principle of visual alignment measurement for axis straightness.

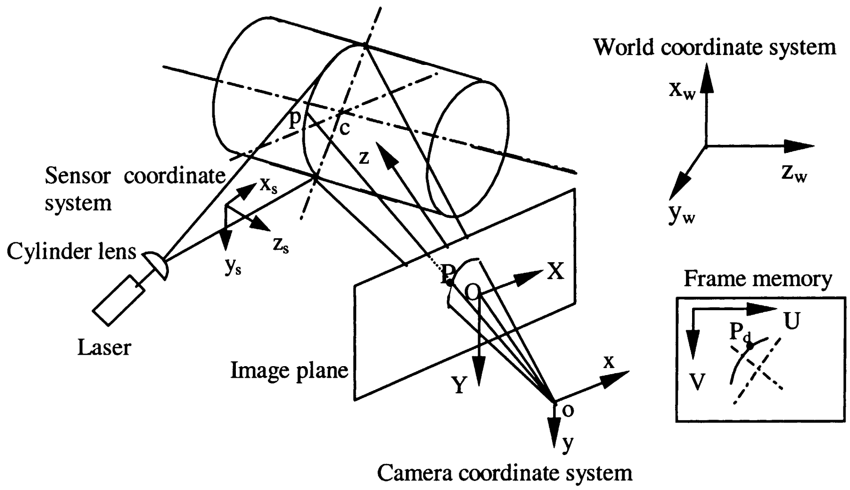

Fig. 2. The measurement principle of the center of ellipse arc by the visual sensor.

coordinate system is P(*X*, *Y*), and the true (distorted) coordinate on the image plane is $P_d(X_d, Y_d)$. The $p_d(U, V)$ is the corresponding row and column numbers of the image pixel in computer frame memory. (U_0, V_0) denotes the pixel position of the principle point O in computer frame memory. Thus, the relations between the coordinate of the point p in the world coordinate system and pixel position $p_d(U, V)$ in computer frame memory can be computed in two steps as given in the following.

2.1. Relation between image coordinate system and sensor coordinate system

As illustrated in Fig. 2, the central axis' x_s and y_s are on the light plane, the equation of which in the sensor coordinate system is $z_s = 0$. Suppose that the rotation and translation vector of x_s and y_s axis in the sensor coordinate system to the camera coordinate system is known as, $(r_2, r_5, r_8)^T$ and $(t_x, t_y, t_z)^T$. The number of CCD sensor pixels in the *X*-direction is N_{cx}, and the center to center distance between adjacent pixels in CCD image plane is d_x in *X*- (scan line) direction; the number of CCD sensor pixels in the *Y*-direction is N_{cy}, and the center to center distance between adjacent sensor pixels in *Y*-direction is d_y. During scanning, the discrete signals picked up by each row of the sensor pixel array are firstly converted to an analog signals, which is then sampled by the computer image grabber into a number of discrete samples and put in a row of a frame buffer. Usually, there exists imperfect match between the computer image grabber and the camera hardware. So uncertainty scale factor S_x should be introduced, which is the ratio between the number of CCD sensor pixels in a row array and the number of picture pixels in a row of the computer image frame memory. The vertical scale factor needs no calibration since there is an exact one-to-one correspondence between lines in the computer frame memory to lines in the CCD sensor array. Therefore, the equation relating the image coordinate system to the sensor coordinate system is as follows

$$\begin{cases} d' = d_x N_{cx}/N_{fx} \\ X_d = s_x^{-1} d'(U - U_0) \\ Y_d = d_y(V - V_0) \\ r = \sqrt{X_d^2 + Y_d^2} \\ f\dfrac{r_1 x_s + r_2 y_s + T_x}{r_7 x_s + r_8 y_s + T_z} = X_d(1 + k_1 r^2 + k_2 r^4) \\ f\dfrac{r_4 x_s + r_5 y_w + T_x}{r_7 x_s + r_8 y_s + T_z} = Y_d(1 + k_1 r^2 + k_2 r^4) \end{cases} \tag{1}$$

where N_{fx} is the number of pixels in a line sampled by the computer, k_1 and k_2 the radial distortion coefficients of CCD camera lens.

2.2. Relation between sensor coordinate system and world coordinate system

As shown in Fig. 2, if the rotation vector $(R_1, R_4, R_7)^T$, $(R_2, R_5, R_8)^T$ and translation vector $(t_x, t_y, t_z)^T$ between sensor coordinate system and world coordinate system is known, $p(x_w, y_w, z_w)$ in the world coordinate system can be obtained from $p(x_s, y_s, 0)$ in the sensor coordinate system. The computation matrix is

$$\begin{bmatrix} x_w \\ y_w \\ z_w \end{bmatrix} = \begin{bmatrix} R_1 & R_2 & T_x \\ R_4 & R_5 & T_y \\ R_7 & R_8 & T_z \end{bmatrix} \begin{bmatrix} x_s \\ y_s \\ 1 \end{bmatrix} \tag{2}$$

3. Computation of the elliptic arc center

In practical measurement, the digital image of elliptic arc as shown in Fig. 3 can be acquired after the image of ellipse arc formed by the intersection between the light plane and the cylinder is sampled by image grabber and computer. Then each point's coordinate of the elliptic arc in the frame

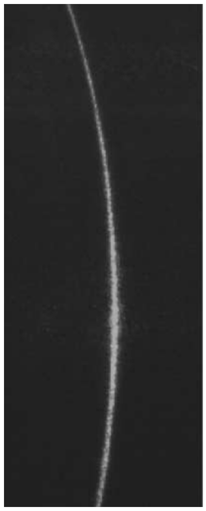

Fig. 3. Digital image of elliptical arc.

memory can be computed through image processing. Suppose the coordinate of elliptic arc center, which is the intersection between light plane and axis, is c(x_w, y_w, z_w) in the world coordinate system, and c(x_{cs}, y_{cs}, 0) in the sensor coordinate system. The corresponding perspective coordinate in the frame memory is $C(u, v)$. In theory, the coordinate of the point c in world coordinate system can be given as follows. First calculate the coordinate $C(u, v)$ in frame memory with the points coordinates of the elliptic arc in the frame memory by image processing. Then using the Eqs. (1) and (2), one can compute its corresponding world coordinate c(x_w, y_w, z_w). But in practice, because the pin-hole perspective model of CCD camera is a non-linear projection, this method gives significant systematic error [11]. Therefore, a better and more accurate algorithm is to use the following. First obtain each point's coordinate p(x_s, y_s, 0) of the elliptic arc in the sensor coordinate system by using Eq. (1), then calculate the coordinate c(x_{cs}, y_{cs}, 0) of the center of elliptic arc in the sensor coordinate system. Although there are many methods to compute the center coordinates and its diameter [12–14], the computation time and accuracy have been major problems, especially for during 100% on-line measurement for large objects. Straightness measurement of seamless steel pipe is such a case, where with a length of 15 m the maximum allowable measurement time is 10 min. So during on-line measurement it is desirable to use least square fifing method to calculate these parameters. In practice, it is very difficult to accurately calculate the center coordinates c(x_{cs}, y_{cs}, 0) in the sensor coordinate system with the small arc as shown in Fig. 3, due to the noise in the curve image. The influence to the curve image by the noise tends to be larger in horizontal direction than that in the vertical one, since the re-sampling of the video signal of the CCD camera is carried out row by row. As a result, the arc becomes a parabola rather than an elliptic arc. Therefore, we place the visual sensors at the two sides of the seamless steel pipe along its axis as illustrated in Fig. 4. Two visual sensors form a group, and the planes of the laser lights are adjusted to make them co-planar. The two sensor coordinate systems in the light plane thus coincide. On the light plane, we can obtain two back projection arcs obtained by the group of two visual sensors. As the two arcs in an ellipse circle act as a geometric constraint in space, we can now compute the center coordinates c(x_{cs}, y_{cs}, 0) accurately and speedily by means of least square fitting method.

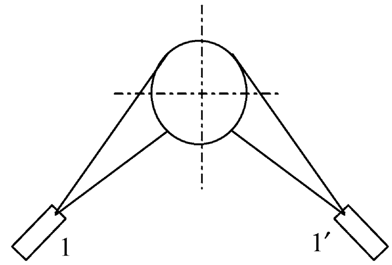

Fig. 4. Arrangement of visual sensors.

If an ellipse is described by the general conic equation

$$Ax^2 + Fxy + By^2 + Cx + Dy + 1 = 0 \tag{3}$$

the coordinate computation equation is

$$x_{cs} = \frac{DF - 2BC}{4AB - F^2}, \qquad y_{cs} = \frac{CF - 2AD}{4AB - F^2},$$
$$R = \sqrt{\frac{AD^2 + BC^2 - CDF + 4AB - F^2}{2(AB - F^2/4)(A + B + \sqrt{(A-B)^2 + F^2})}} \tag{4}$$

where R is the short axis length of the elliptic arc, which is the diameter of the ellipse formed by the light plane intersecting the measured seamless steel pipe. A, B, F, C and D can be obtained by Eq. (5)

$$\begin{bmatrix} A \\ B \\ F \\ C \\ D \end{bmatrix} = \begin{bmatrix} \sum_{i=0}^{n-1} x_{si}^4 & \sum_{i=0}^{n-1} x_{si}^2 y_{si}^2 & \sum_{i=0}^{n-1} x_{si}^3 y_{si} & \sum_{i=0}^{n-1} x_{si}^3 & \sum_{i=0}^{n-1} x_{si}^2 y_{si} \\ \sum_{i=0}^{n-1} x_{si}^2 y_{si}^2 & \sum_{i=0}^{n-1} y_{si}^4 & \sum_{i=0}^{n-1} x_{si} y_{si}^3 & \sum_{i=0}^{n-1} x_{si} y_{si}^2 & \sum_{i=0}^{n-1} y_{si}^3 \\ \sum_{i=0}^{n-1} x_{si}^3 y_{si} & \sum_{i=0}^{n-1} x_{si} y_{si}^3 & \sum_{i=0}^{n-1} x_{si}^2 y_{si}^2 & \sum_{i=0}^{n-1} x_{si}^2 y_{si} & \sum_{i=0}^{n-1} x_{si} y_{si}^2 \\ \sum_{i=0}^{n-1} x_{si}^3 & \sum_{i=0}^{n-1} x_{si} y_{si}^2 & \sum_{i=0}^{n-1} x_{si}^2 y_{si} & \sum_{i=0}^{n-1} x_{si}^2 & \sum_{i=0}^{n-1} x_{si} y_{si} \\ \sum_{i=0}^{n-1} x_{si}^2 y_{si} & \sum_{i=0}^{n-1} y_{si}^3 & \sum_{i=0}^{n-1} x_{si} x_{si}^2 & \sum_{i=0}^{n-1} x_{si} y_{si} & \sum_{i=0}^{n-1} y_{si}^2 \end{bmatrix}^{-1} \begin{bmatrix} \sum_{i=0}^{n-1} x_{si}^2 \\ \sum_{i=0}^{n-1} y_{si}^2 \\ \sum_{i=0}^{n-1} x_{si} y_{si} \\ \sum_{i=0}^{n-1} x_{si} \\ \sum_{i=0}^{n-1} y_{si} \end{bmatrix} \tag{5}$$

After the coordinate of point c in the sensor coordinate system and the diameter R of axes are obtained using Eqs. (4) and (5), the coordinate of c(x_w, y_w, z_w) in the sensor coordinate system can be given by Eq. (2). Thus, according to the straightness evaluation principle, the straightness of seamless steel pipe can be obtained by using the evaluation method given in [8].

4. Calibration of the alignment system

From Eqs. (1) and (2), we know that there are 24 unknowns in the measured model. They are the effective focal length of the camera f, uncertainty scale factor s_x, the coordinates of the optical center O in the image coordinate system (U_0, V_0), the coefficients of radial distortion k_1 and k_2, the rotation vector $(r_2, r_5, r_8)^{\mathrm{T}}$ and translation vector $(t_x, t_y, t_z)^{\mathrm{T}}$ between sensor coordinate system and camera coordinate system, and the rotation vector $(R_1, R_4, R_7)^{\mathrm{T}}$, $(R_2, R_5, R_8)^{\mathrm{T}}$ and translation vector $(T_x, T_y, T_z)^{\mathrm{T}}$ between sensor coordinate system and world coordinate system. These unknown parameters can be extracted by the internal and external calibration of the visual sensor. The parameters f, s_x, U_0, V_0, k_1, and k_2, which are internal unknowns of camera, are calibrated by the internal calibration. Up to now there are many methods for the calibration. The basic principle lies in using the coordinates of the 3D or 2D target in a world coordinate system and their correspondences in the image coordinate system, to extract these parameters by some linear or nonlinear optimal method according to Eqs. (1) and (2). Among these methods, the most popular one is Tsai's RAC calibration method [11,12]. The other 18 parameters of the rotation and translation vectors, which are external parameters of visual sensor, can be extracted by external or global calibration. This calibration scheme is illustrated in Fig. 5 [1]. Firstly, use the calibration target which consist of three thin wires to generate three non-collinear points on the light plane. Next, calculate these points' coordinates, both in the world or global coordinate system (GCS), or in theodolite coordinate system (TCS) by two theodolites, and in the sensor coordinate system (SCS) by sensors and image processing. Then compute the rotation vector $(R_1, R_4, R_7)^{\mathrm{T}}$, $(R_2, R_5, R_8)^{\mathrm{T}}$ and translation vector $(T_x, T_y, T_z)^{\mathrm{T}}$ by solving the non-linear equations or least square fitting according to Eq. (2). Lastly, with the internal parameters of the camera and those points' coordinates in the image coordinate system, extract the rotation vector,$(r_2, r_5, r_8)^{\mathrm{T}}$ and translation vector $(t_x, t_y, t_z)^{\mathrm{T}}$ by the optimization method.

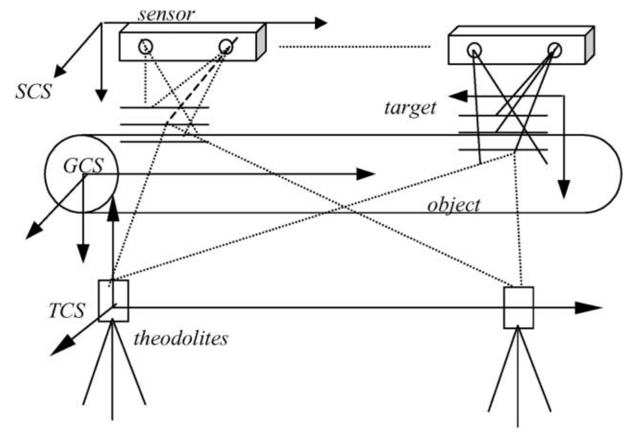

Fig. 5. Global calibration of measuring system.

5. Experimental results

In order to test the proposed method and obtain the measurement precision of the visual alignment measurement technique presented previously, we built a set-up of visual alignment experiment system as shown in Fig. 6. Using three visual sensor groups, each of the group consisting of two sensors arranged at the two sides. The camera used here is Mintron MTV-368P. The center to center distance between two adjacent sensor elements in X-direction $d_x = 0.980$ μm, and in Y-direction $d_y = 0.6357$ μm. The nominal focal length of the camera lens f is 25 mm. The sampling range of the image grabber is 512 pixels × 512 pixels. The arrangement of sensors on one side is given in Fig. 1. The result of internal and external calibrations of the measurement

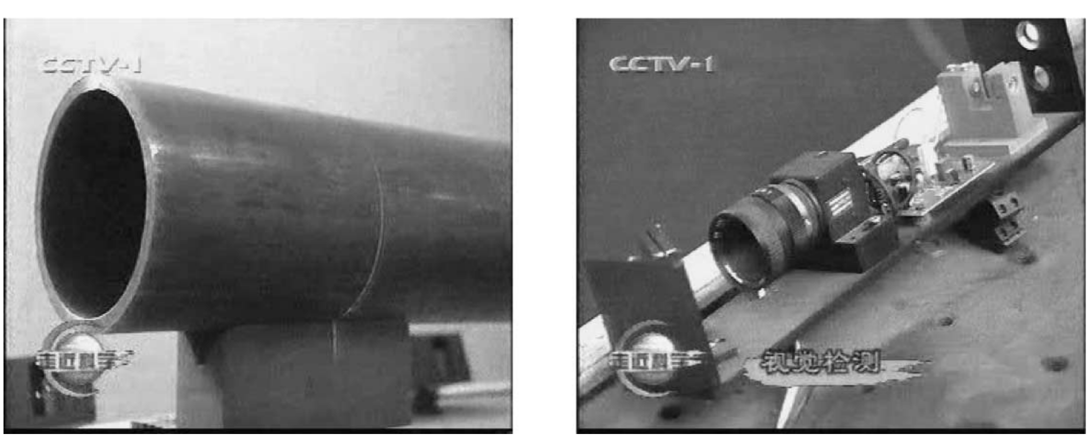

Fig. 6. Visual alignment system for seamless steel pipe.

Table 1
The calibration result of the visual alignment measurement system

Parameter type	Parameter	Sensor no. 1	Sensor no. 1′	Sensor no. 2	Sensor no. 2′	Sensor no. 3	Sensor no. 3′
Camera internal parameter	f	26.945040	28.455259	26.877989	28.744300	26.932296	28.492267
	U_0	240.627832	275.133136	262.679271	253.278782	220.190476	291.046543
	V_0	284.216627	286.700176	272.081798	261.650528	295.810156	277.663119
	d_x	0.009800	0.009800	0.009800	0.009800	0.009800	0.009800
	d_y	0.006357	0.006357	0.006357	0.006357	0.006357	0.006357
	s_x	1.547011	1.547024	1.550284	1.557109	1.553885	1.549453
	k_1	−7.913685 e-4	−7.0 e-6	−3.445633 e-4	−2.247 e-3	−7.653260 e-4	−5.20 e-4
Transform matrix between camera coordinate system and sensor coordinate system	r_1	−0.051598	0.168624	−0.000966	0.182522	0.025760	0.170669
	r_4	0.982783	0.967912	0.994115	0.950247	0.998439	0.930676
	r_7	0.177411	−0.186309	0.108327	−0.252423	0.049556	−0.323596
	r_2	−0.531245	0.168430	−0.537434	0.231531	−0.510522	0.241158
	r_5	−0.177439	0.157941	−0.091869	0.207974	−0.029481	0.278969
	r_8	0.828429	0.972978	0.838287	0.950337	0.859359	0.929523
	t_x	12.754174	0.709845	10.427927	14.61684	15.498480	11.301432
	t_y	−28.434310	−41.000171	−30.548719	−45.914128	−30.535456	−37.481670
	t_z	546.788768	750.293259	553.807162	858.579454	560.052618	926.523729
Transform matrix between sensor coordinate system and world coordinate system	R_1	0.011228	0.011228	0.018966	0.018966	0.022528	0.022528
	R_4	0.980430	0.980430	0.967887	0.967887	0.954388	0.954388
	R_7	0.196546	0.196546	0.250668	0.250668	0.297717	0.297717
	R_2	−0.027269	−0.027269	−0.026606	−0.026606	−0.024695	−0.024695
	R_5	0.196786	0.196786	0.251113	0.251113	0.298233	0.298233
	R_8	−0.980067	−0.980067	−0.967592	−0.967592	−0.954174	−0.954174
	T_x	962.210008	962.210008	1591.472390	1591.472390	2154.531287	2154.531287
	T_y	415.856972	415.856972	418.311535	418.311535	420.403840	420.403840
	T_z	2218.801544	2218.801544	2218.744659	2218.744659	2218.691864	2218.691864

system is given in Table 1. From the table, we can see that the effective focal length of the camera is not equal to the nominal one, and there is an offset of the image center from the camera's optical center. As shown in Table 1, the offset in the vertical direction can be as much as 40 pixels. The radial distortion coefficient k_1 is enough to satisfy the precision requirement, the magnitude order of which is 10^{-4}. After the alignment measurement system was calibrated, we measured the straightness of a seamless steel pipe, whose nominal radius is 70 mm and length 1500 mm. The visual sensor is 400 mm away from the pipe. For the same circumference measurement, the measurements were taken at the same time. The measurement results as shown in Table 2 were obtained for every 75° when circumrotated. The straightness of the pipe is obtained by least square fitting. With this method, we first obtain the least square base line,

Table 2
Result of straightness

Time	Number	x_w	y_w	z_w	R	Straightness
1	1	963.872	415.385	2276.283	69.956	0.565
	2	1593.196	420.492	2274.356	69.814	
	3	2156.255	424.994	2273.434	69.719	
2	1	963.882	415.278	2276.669	69.893	0.527
	2	1593.210	420.240	2274.931	69.780	
	3	2156.274	424.979	2274.064	69.735	
3	1	963.875	415.190	2276.440	69.901	0.559
	2	1593.200	420.123	2274.623	69.817	
	3	2156.262	424.774	2273.756	69.747	
4	1	963.870	415.133	2276.270	69.972	0.571
	2	1593.197	420.291	2274.469	69.813	
	3	2156.259	424.793	2273.662	69.730	
5	1	963.871	415.454	2276.251	70.090	0.563
	2	1593.201	420.665	2274.465	69.791	
	3	2156.263	425.105	2273.636	69.685	

and next calculate the offset of every point coordinate along the pipe centerline from the base line. Then we calculate the maxim offset. Thus, the pipe's straightness can be evaluated as twice of the maxim offset. From Table 2, we observe that the measurement mean value is 0.557 mm with a standard deviation of 0.015 mm. In order to estimate the measurement precision of the alignment measuring system, we used a CMM to measure the pipe straightness and obtained the result of 0.50 mm. Therefore, our measurement precision for the alignment is tested to better than 0.06 mm.

6. Conclusion

The visual alignment system presented above proved to be successful in the experiments. In practice, in order to obtain high measurement precision, no less than three visual sensor groups along the axes to be measured should to be used. With more measurement points used, a higher measurement precision is achievable when the pipe straightness is evaluated. For the 1500 mm long seamless steel pipe, more than five sensor groups are advisable. From the result as shown in Table 2, we can observe that the experimental device is quite high in precision. Even so, better precision is still achievable. In this experimental system, due to the limitation of worktable size, the distance between sensor and the pipe was set only to 400 mm. The focal length of the camera, which is 25 mm, is a bit bigger. The measurement field of view at 400 mm from the camera is only about 50 mm, which can cover only 1/8 of the pipe's circumference with the corresponding central angle form the pipe central line being about 40°. If the focal length of the camera is smaller, such as 8–16 mm, the central angle of the covered scope will be bigger than 90°, and the measurement precision would be improved. The trace to the source of the measurement precision base is a steel ruler of 1000 mm long in the global calibration. If a high precision invar ruler is used, and a precise calibration target is used, more accurate calibration precision can be obtained. Furthermore, the single measurement time of this experimental system is shorter than 2 s, while that of CMM (including the fixing time of the pipe) is about 10 min. Therefore, the developed method and system offers its unique advantage over the traditional methods for the straightness measurement of seamless steel pipe whose the product time is only a few tens of seconds. Thus, it can be concluded that the laser visual alignment measurement technique is an important method for on-line and non-contact measurement. It cannot only fulfil 100% on-line measurement, but also gives high measurement precision.

References

[1] R. Lu, Study on the Visual Alignment Technique for On-line Measurement, The Research Report of Postdoctoral Research, Tianjin University, China, 2000.
[2] D. Vernon, Machine Vision — Automated Visual Inspection and Robot Vision, Cambridge University Press, Cambridge, 1991.
[3] F.T. Farago, M.A. Curtis, Handbook of Dimensional Measurement, 3rd Edition, Industrial Press Inc., 1994.
[4] U. Junichi, S. Shimada, N. Ikawa, A. Komura, Straightness measurement using laser beam straight datum, SPIE Int. Soc. Opt. Eng. 2576 (1995) 315–322.
[5] M. Sasaki, H. Takebe, K. Hane, Transmission-type position sensor for the straightness measurement of a large structure, J. Micromech. Microeng. 9 (4) (1999) 429–433.
[6] Z. Ge, Q. Min, Z. Jiao, X. Zeng, Photoelectric automatic three-dimension straightness instrument, SPIE Int. Soc. Opt. Eng. 2899 (1996) 131–140.
[7] W.B. Herrmannsfeldt, M.J. Lee, J.J. Spranza, K.R. Trigger, Precision alignment using a system of large rectangular fresnel lenses, selected papers on zone plates, SPIE Milestone Ser. MS128 (1996) 212–222.
[8] G. Henzold, Handbook of Geometrical Tolerancing, Design, Manufacturing and Inspection, Wiley, New York, 1995.
[9] R.Y. Tsai, A versatile camera calibration technique for high-accracy 3D machine vision metrology using off-the-shelf TV cameras and lenses, IEEE J. Robot. Automation RA-3 (4) (1987) 323–344.
[10] R.Y. Tsai, An efficient and accurate camera calibration technique for 3D machine vision, in: Proceedings of the IEEE Conference on Computer Vision and Pattern Recognition, Miami Beach, FL, 1986, pp. 364–374.
[11] J. Heikkila, Accurate camera calibration and feature based 3D reconstruction from monocular image sequences, Ph.D. dissertation, University of Oulu, Finland, 1997.
[12] P.L. Rosin, Further five-point fit ellipse fitting, Graph. Models Image Proc. 61 (1999) 245–259.
[13] C. Daul, P. Graebling, E. Hirsch, From the Hough transform to a new approach for the detection and approximation of elliptical arcs, Graph. Models Image Proc. 72 (3) (1998) 215–236.
[14] E.R. Davies, Machine Vision: Theory, Algorithms, Practicalities, Academic Press, London, 1990.